

See discussions, stats, and author profiles for this publication at: <https://www.researchgate.net/publication/235782097>

Surface Induced Order of Solution Processed Caffeine Needles on Silica and Muscovite Mica

ARTICLE *in* CRYSTAL GROWTH & DESIGN · JANUARY 2013

Impact Factor: 4.89 · DOI: 10.1021/cg301812m

CITATIONS

7

READS

39

6 AUTHORS, INCLUDING:



[Oliver Werzer](#)

Karl-Franzens-Universität Graz

55 PUBLICATIONS 777 CITATIONS

[SEE PROFILE](#)



[Eva Roblegg](#)

Karl-Franzens-Universität Graz

67 PUBLICATIONS 571 CITATIONS

[SEE PROFILE](#)



[Andreas Zimmer](#)

Karl-Franzens-Universität Graz

134 PUBLICATIONS 2,375 CITATIONS

[SEE PROFILE](#)



[Martin Oehzelt](#)

Helmholtz-Zentrum Berlin

87 PUBLICATIONS 1,651 CITATIONS

[SEE PROFILE](#)

Surface Induced Order of Solution Processed Caffeine Needles on Silica and Muscovite Mica

O. Werzer,^{*,†} B. Kunert,[§] E. Roblegg,^{†,‡} A. Zimmer,[†] M. Oehzelt,^{†,||} and R. Resel[§]

[†]Institute of Pharmaceutical Sciences, Department of Pharmaceutical Technology, Karl-Franzens University Graz, 8010 Graz, Austria

[‡]Research Center Pharmaceutical Engineering GmbH, 8010 Graz, Austria

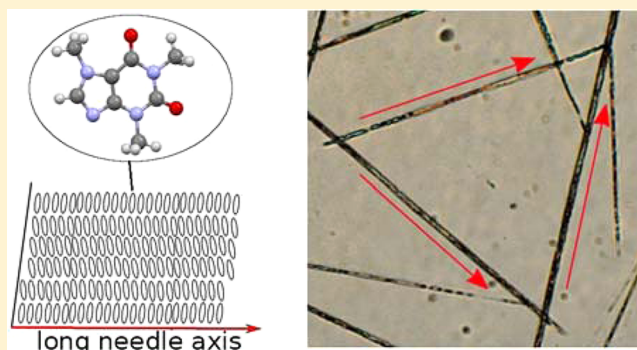
[§]Institute of Solid State Physics, Graz University of Technology, 8010 Graz, Austria

^{||}Humboldt-Universität zu Berlin, Institut für Physik, D-12489 Berlin, Germany

^{||}Helmholtz Zentrum Berlin für Materialien und Energie, BESSY II, D-12489 Berlin, Germany

Supporting Information

ABSTRACT: In this work the orientational order of needle-shaped caffeine crystallites at silica and muscovite mica surfaces is investigated by X-ray diffraction experiment and optical microscopy. The investigation of thin films reveals the formation of caffeine in the anhydrous monoclinic β -polymorphic structure independent of the surface with the dislike caffeine molecules assemble in an edge-on conformation. The silica surface provides isotropic properties for crystal growth which leads to a fiber texture arrangement of the needles; a majority of needles have a 010 texture with all other directions being randomly distributed. The mica surface with its highly regular surface structure induces defined textures and azimuthal order of the caffeine needles resulting in a fully defined epitaxial order. The edge-on and dislike caffeine molecules align along the $[100]_m$, $[110]_m$, and $[1\bar{1}0]_m$ real space directions of the mica substrate and show a mirror symmetry around the $[110]_m$. The experiments on these two surfaces show that the type of surface is able to induce order during caffeine needle growth.



1. INTRODUCTION

Organic molecule deposition on solid templates is used in a variety of fields including pharmaceuticals,¹ food industry,² colloid science,^{3,4} organic electronics,^{5,6} among others. Within pharmaceutical applications limited solubility and stability are overcome by the introduction of solid nanoparticle surfaces made from PLGA,^{7,8} gelatin,^{9,10} or nanolipid nano carriers¹ which are coated with drug molecules. These surface modifications provide improved stability, dissolution properties, and the ability for drug targeting but also influences the toxicity within the living organisms.^{11,12}

The introduction of a solid boundary condition directly impacts the crystal growth as molecules not only arrange on the account of molecule–molecule interactions within the material but also due to various interactions with the surface (van der Waal, H-bonding, or electrostatics).¹³ Furthermore, the substrate surface order has a decisive impact on the growth properties. On isotropic surfaces, strong texturing in one direction is observed; typically one contact plane of the crystal with the surface exists, while all other crystal planes are azimuthally random distributed.¹⁴ On the introduction of anisotropic surfaces like rubbed polyimide surfaces uniaxially in-plane order (azimuthal alignment) is imposed,^{15,16} as anisotropic anchor energies favor the alignment along defined

directions.¹⁷ Single crystal surfaces made from mica,^{18,19} copper,²⁰ KCl,²¹ rutile,²² or others provide periodic surface properties allowing even for epitaxial order (out-of plane and azimuthal order).²³ Besides the surface interactions, the thermodynamic and kinetic process conditions are of crucial importance for the crystal growth which even allow for the induction of surface mediated polymorphic structures typically not observable in bulk material.^{5,14,24} The formed layers have defined morphological (size, shape) and crystallographic film properties which can be expected to impact directly, for instance, the dissolution properties.

Typically, the uniaxial alignment or epitaxial growth of organic molecules on anisotropic surfaces requires the usage of several processing steps; often high-vacuum conditions or heat treatments are necessary for the achievement of defined directional crystal growth which often requires much effort. Within this work the crystalline microstructure of the asymmetric and dislike molecule caffeine on silica and muscovite mica is investigated. Thin films are prepared via a solution based drop cast technique, which promises to be a

Received: December 11, 2012

Revised: January 18, 2013

Published: January 22, 2013

reproducible and cost-/resource-efficient production process. While the silica surface is an isotropic surface, the mica surface provides highly symmetric surface properties for the alignment of caffeine molecules during crystallization. The samples are investigated by optical microscopy to determine the influence of the substrate surfaces on the morphology of the formed crystals. Various X-ray diffraction experiments are used to determine the crystal phases and their orientational order with respect to the substrate surfaces.

2. EXPERIMENTAL METHODS

Anhydrous caffeine powder of pharmaceutical grade was purchased from Herba Chemosan-AG (Vienna, Austria) and used without further modification. The chemical structure of the molecule is provided in the inset of Figure 1. Two sets of samples were prepared. For powder

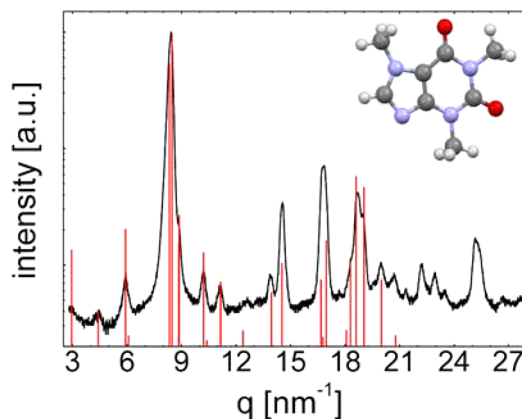


Figure 1. X-ray powder diffraction pattern of anhydrous caffeine. Peak positions and relative intensities of the caffeine β -phase generated from literature values²⁸ (vertical lines). Inset shows chemical structure of the caffeine molecule consisting of carbon (dark gray), nitrogen (blue), oxygen (red), and hydrogen (gray).

investigations, caffeine was dissolved with 30 mg/mL in tetrahydrofuran (THF) and heated to 50 °C resulting in fully dissolved caffeine. The solution was cooled to ambient temperatures followed by solvent removal via rotary evaporation at a pressure of 40 mbar. The obtained crystalline powder was then used without further treatment.

The second set of samples are caffeine thin films. For the preparation of these films, caffeine was dissolved at room temperature at concentration of 2 mg/mL in THF. Two different substrates were used. Single crystal silicon wafers with a top layer of thermal silicon oxide layer of about 100 nm were used as isotropic silica surfaces. The substrates were cleaned in a surfactant solution containing NaOH, rinsed with Milli-Q water and ethanol, and finally dried under a nitrogen stream. Muscovite mica surfaces were prepared by cleavage of the crystal prior to the film deposition providing a clean surface for the experiments. Thin films were obtained via drop casting. Drops of 30 μL were placed on $1.5 \times 1.5 \text{ cm}^2$ substrates and covered with a Petri dish resulting in an evaporation time of about 1 min for all samples.

X-ray powder diffraction, specular X-ray diffraction, and rocking curves measurements were performed with a Panalytical Empyrian reflectometer equipped with a copper sealed tube (wavelength $\lambda = 0.154 \text{ nm}$), a primary side multilayer mirror providing a parallel beam, a secondary side slit optic system, and a PiXcel detector. X-ray diffraction powder scans and specular scans were performed by symmetric variations of the incident and exit angles resulting in the scattering vector remaining normal to the silica surface at all times. The angular measurement (θ) is transformed to the scattering vector (q) notation by $q = 4\pi \sin(\theta)/\lambda$. Rocking curve scans are performed by rotating the sample around the vertical direction. This results in the scattering vector having the same length, but its direction is changed with respect of the surface normal during a rocking scan.

X-ray diffraction pole figure²⁵ experiments were performed with a Philips X'Pert diffractometer equipped with an ATC3 texture cradle. X-ray radiation was generated using a sealed chromium tube providing a wavelength of 0.229 nm which is further improved by a secondary side graphite monochromator. In general X-ray diffraction pole figures (XRD-PF) represent the diffracted intensities for specific d -spacings as function of the Euler angles ϕ and ψ ; ϕ is the rotation around the sample surface normal and ψ denotes the inclination to the surface normal.²⁵ The data are depicted in polar contour plots with ϕ as the polar angle, ψ as the polar radius, and the intensity color coded.²⁶ Enhanced intensities correspond to Bragg reflections in certain directions and are denoted as poles with the netplanes being normal to the poles. The experimental data were evaluated with the software package Stereopole,²⁷ providing information on the orientational order of the observed crystal phase.

Optical microscopy images were taken with an Axiovert 40 microscope (Zeiss, Germany) equipped with a high resolution digital camera.

3. RESULTS

3.1. XRD of Caffeine Powder. A qualitatively X-ray powder diffraction scan of recrystallized caffeine powder is shown in Figure 1. The pattern reveals numerous peaks over the entire scan range typical for a powder sample with randomly distributed crystallites. The most dominant peaks are located at 8.4 nm^{-1} , 14.5 nm^{-1} , 16.8 nm^{-1} , and 18.8 nm^{-1} corresponding to d -spacings of 0.74 nm, 0.43 nm, 0.37 nm, and 0.33 nm, respectively. A comparison reveals an excellent agreement between the experimental and theoretical peak positions of caffeine in the anhydrous β -phase²⁸ with a monoclinic unit cell of $a = 4.30 \text{ nm}$, $b = 1.51 \text{ nm}$, $c = 0.70 \text{ nm}$, and $\beta = 99.03^\circ$. Some deviation of the peak intensities between the literature values and the experimental data is present. As caffeine forms needle-like crystallites texturing within the sample occurs; i.e., the crystallites within the powder are not entirely randomly oriented, and an alignment of the crystallites with its long axis parallel to the surface is expected to be more likely which results in relative peak heights being different to a perfect powder sample.

3.2. Optical Microscopy of Caffeine Needles on Surfaces. Thin films of caffeine from THF solutions on mica and silica surfaces were prepared via a drop casting process revealing the formation of needle-like crystallites lying along the substrate surfaces (see Figure 2). On the silica surface (Figure 2a) the needles length vary from a couple of micrometers to millimeter range. The needles show a random azimuthal distribution; i.e., no preferred orientation can be identified.

As the surface is changed to mica, needle growth of caffeine is preserved but other than on silica preferred alignment directions of the needles are noticeable (see Figure 2b) with typical angles with respect to each other. For instance, an inclination of 60° is observed for some contacting needles forming a regular triangle as indicated by labels 1, 2, and 3 within the microscopy image. Such symmetry is expected as the mica surface provides a 120° surface symmetry, meaning that the surface structure is equivalent in three azimuthal directions within the substrate surface. Another often observed inclination angle is 18° as indicated for needles at the point labeled as 4. Such an angle is a consequence from the caffeine unit cell being monoclinic with $\beta = 99^\circ$; inverting a needle upside down with respect of the surface results in a similar needle which is rotated by 18° with respect of the first orientation and will be discussed further below.

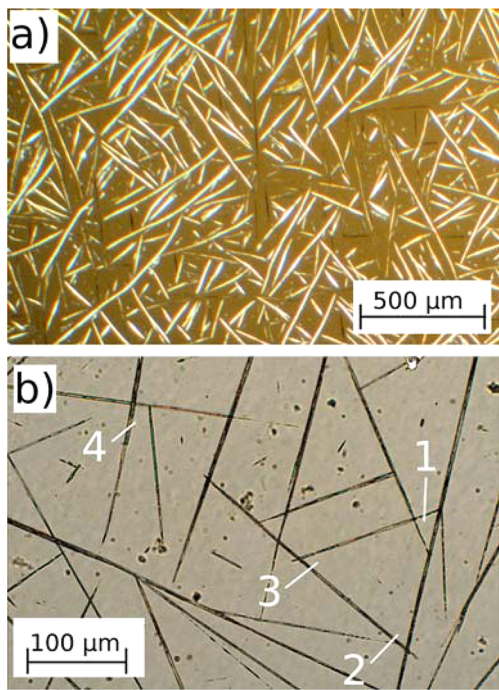


Figure 2. Optical microscopy images of caffeine drop cast on silica (a) and mica (b) surfaces. Labels 1–4 indicate commonly observed angles between needles.

3.3. Specular X-ray Diffraction and Rocking Curves. Specular X-ray diffraction patterns from drop cast caffeine thin films are shown in Figure 3a. Such scans provide information on crystallographic net planes (contact planes) which are

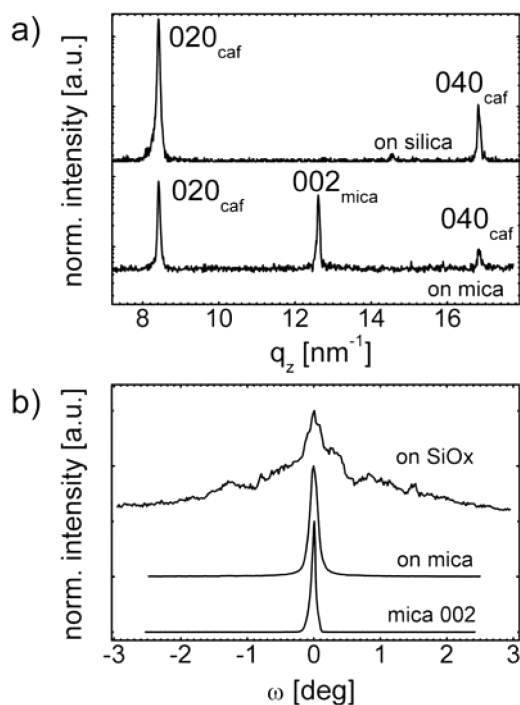


Figure 3. (a) Specular X-ray diffraction pattern of crystalline caffeine on silica and on mica with indexation of the diffraction peaks. (b) X-ray diffraction rocking curve measurements of the 020 caffeine reflection of needles on silica and mica, and the 002 peak of mica substrate. Curves are shifted for clarity.

parallel to the surface. For the sample prepared on silica two peaks located at 8.4 nm^{-1} and 16.8 nm^{-1} are observed corresponding to the 020 and 040 net planes of caffeine in accordance with the crystallites having a 010 contact plane with the silica surface. For the identification of the mosaicity of the 020 net planes, i.e., the quality of the crystal orientation with respect of the surface, a X-ray diffraction rocking curve measurement is performed. Such a scan allows identification of the angular distribution of crystallites with respect of the surface normal ($\omega = 0^\circ$). The measurement reveals maximal intensity at $\omega = 0^\circ$ (see Figure 3b) corresponding to the specular direction with surface parallel netplanes. However, as the intensity is collected off the specular direction a broad diffuse background can be identified which even has small peaks at $\omega = -1.2^\circ, -0.8^\circ, -0.1^\circ, 0.08^\circ, 0.4^\circ, 0.8^\circ$, and 1.5° . This suggests that the majority of caffeine crystallites have a 010 orientation/texture, but that fractions of the caffeine crystallites are tilted from the surface normal.

The same set of measurements performed on a caffeine sample prepared on a mica surface reveals a similar behavior for the specular direction but distinct properties in the rocking curve scans. Within the specular scan the 020 and 040 reflections are present showing that these needles have the same 010 texture. In addition a Bragg peak at 12.6 nm^{-1} occurs, which corresponds to the 002 peak of the silicate sheet repeating distance of mica. Peaks corresponding to other interplanar distances are not detected within this scan. The rocking curve measurement on the 020 reflection reveals a single sharp peak without a noticeable background suggesting that the mosaicity is strongly reduced (Figure 3b); i.e. the quality of the crystal alignment is enhanced compared to the silica surface. The full width at half-maximum of this peak is $\Delta\omega = 0.12^\circ$, which is about twice as broad compared to the rocking width measured on a mica single crystal peak ($\Delta\omega = 0.07^\circ$).

3.4. X-ray Pole Figure Measurements. A pole figure allows determination of the orientational distribution of specific poles with respect of the surface normal (ψ) and the azimuthal direction (ϕ) relative to the substrate. A pole corresponds to a specific d -spacing and is normal on the netplane. Pole figure measurements of caffeine grown on silica for $|q| = 8.4 \text{ nm}^{-1}$ are depicted in Figure 4a. The results show the typical pole density distribution for samples containing a fiber texture with enhanced intensities along constant ψ . The middle of the pole figure corresponds to diffracted intensities from net planes being parallel to the substrate surface, which corresponds to 020 reflections of caffeine also observed within the specular scan (compare Figure 3a). The enhanced intensities at higher ψ -values correspond to 510 net planes, which are inclined by 60.5° to the surface normal. While the inclination to the surface normal is well-defined, preferred orientation in azimuthal direction (along ϕ) is not observed in agreement with the random distribution of needles within the surface. An additional pole figure taken at $|q| = 18.8 \text{ nm}^{-1}$ reveals a similar behavior but with the intensities inclined by 78° from the surface normal corresponding to the -112 of the caffeine crystal in a 010 texture (data are provided as Supporting Information).

The pole figure at $|q| = 8.4 \text{ nm}^{-1}$ for the caffeine crystals prepared on the muscovite mica surface is shown in Figure 4b. Similar to the results obtained from the silica substrate high pole densities intensities are found in the center of the polefigure corresponding to the 020 reflections and at $\psi = 60.5^\circ$ corresponding to the 510 reflection of caffeine. Other than on silica the pole densities are cumulated at around $\phi = 33^\circ, 95^\circ$,

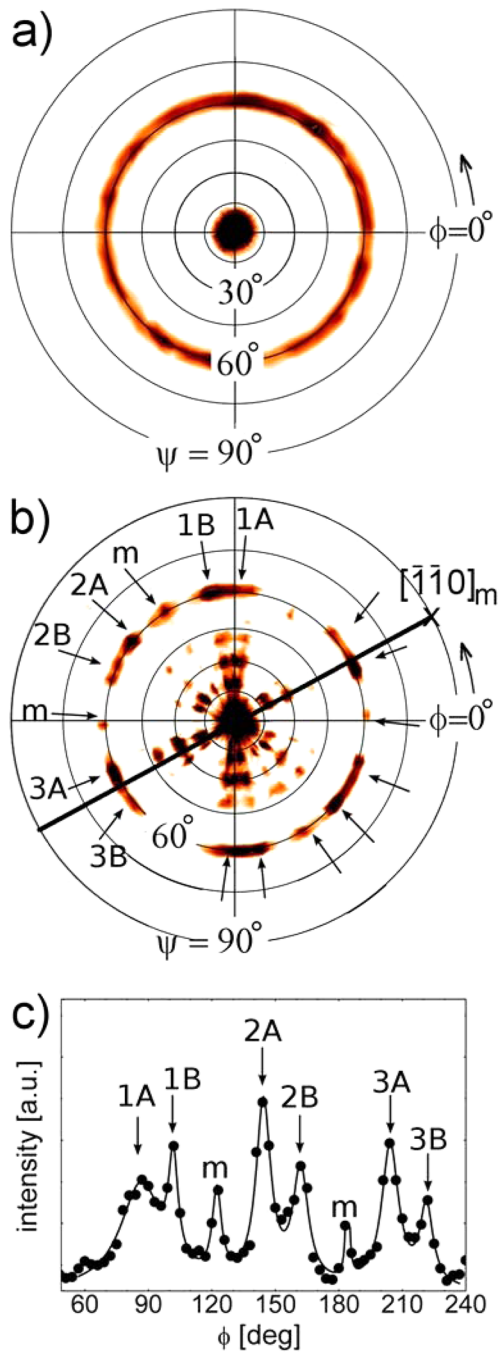


Figure 4. Pole figures taken at $lql = 8.4 \text{ nm}^{-1}$ for caffeine needles on silica (a) and mica (b). Line scan along ϕ at constant $\psi = 60.5^\circ$ performed on the mica sample (c). Labels indicate corresponding positions within the pole figures and the ϕ -scan. m denotes mica poles and $[\bar{1}10]_m$ denote the real space mirror axis of mica.

154°, 214°, 271°, and 328° (indicated by the arrows in Figure 4b) revealing that the crystallites are aligned along certain directions. The poles are about 60° inclined with respect to each other in accordance with the optical microscopy images. The pole density distribution along the azimuth ϕ at constant $\psi = 60.5^\circ$ is shown in Figure 4c. This figure clearly shows that the poles consist of double peaks which are about 18° separated with respect to each other; this angle is similar to the observation in the optical microscopy image (compare Figure 2b label 4). Within the pole figure in Figure 4b additional peaks are found at $\phi = 3^\circ, 123^\circ, 183^\circ$, and 303° and $\psi \sim 60^\circ$, which

are the results of higher harmonic reflections of the underlying mica substrate and are labeled with m . From this the orientation of the mica substrate is obtained showing that the $[\bar{1}10]_m$ axis, a main symmetry axis of mica, point toward $\phi = 33^\circ$ and $\psi = 90^\circ$. All observed reflections of the caffeine needles have a symmetric reflection mirrored at the $[\bar{1}10]_m$ direction, i.e., are inclined by the same amount in ϕ from this axis. (Equivalently, the 180° rotated $[110]_m$ located at $\phi = 213^\circ$ and $\psi = 90^\circ$ can be used as the mirror axis.)

At ψ -values of 20°, 30.6°, 41.5° additional poles are noticed which have the same azimuthal rotations compared to the poles at $\psi = 60.5^\circ$. As the pole figure is taken at $lql = 8.4 \text{ nm}^{-1}$ these poles must correspond to 510 reflections of caffeine crystals with textures deviating from the 020; 110, 520, and 530 texture are able to explain poles with such inclination to the surface.

A pole figure measurement performed at 18.8 nm^{-1} reveals again localized enhanced poles corresponding to the $\bar{1}12$ poles of caffeine needles explainable with the same texture as observed above (data are provided in the Supporting Information).

4. DISCUSSION

Crystallization of caffeine in the presence of THF results in the formation of needles in the β -caffeine polymorphic²⁸ structure which does not contain solvent molecules within the crystal unit cell. All experimental data are explainable with this structure. The formation of a distinct polymorph like the high temperature α -phase with a hexagonal morphology^{29,30} was not observed within the optical and X-ray investigations showing that neither the preparation route nor the substrate induces other polymorphic structures. Furthermore the samples were stable over the course of the experiments (the X-ray investigation took about 48 h) at ambient conditions, and a transformation into a hydrated form³¹ was not detected.

The silica surface consists of silicon and oxygen providing H-bonding and negatively charged sites which are randomly distributed across the surface providing isotropic surface properties for the crystal growth. The muscovite mica surface is a sheetlike silicate consisting of silicon (which are partly substituted by aluminum atoms) and oxygen in a regular dioctahedral regular arrangement. As a result a pseudo 120° symmetry is formed at the surface. However, vacancies within the octahedral layer are present which causes a distortion of the surface atom arrangement and shallow grooves along the $[\bar{1}10]_m$ direction result.³² This results in a mica surface symmetry with a two-dimensional space group cm which provide a mirror symmetry with respect to mica's $[\bar{1}10]_m$ direction.^{33,34}

The microscopy images show that caffeine forms crystallites with needle shapes which are aligned along the surface independent of the nature of the substrate under investigation. From the measurements it cannot be decided if the crystals form in solution or directly at the surface. However, the orientational differences on the two different surfaces show that the surfaces have a decisive influence suggesting a crystal formation at the very interface is present. This means that the caffeine molecules have sufficient adsorption strength to compete with the THF molecules for attachment sites on both surfaces. Besides the differences in the azimuthal alignment of the crystallites, differences in the crystallite size distributions also are noted. Crystallites grown on the silica surface reveal a broader size distribution compared to the crystallites grown on mica. As the silica surface does not

provide periodic surface structures which would provide nucleation sites for the crystal growth, nucleation initiation is most probably taking place at different times leaving the individual crystallite different crystallization times and consequently results in a broader size distribution. In addition, larger crystallites grow faster on account of smaller crystallites in accordance with the Ostwald ripening³⁵ and a majority of larger crystallites are observed.

The caffeine crystals grown from the THF solution have a crystallographic unit cell of $a = 4.30$ nm, $b = 1.5$ nm, $c = 0.69$ nm, and $\beta = 99.03^\circ$. Along the crystal c -axis of the unit cell caffeine molecules (with its “dislike” shape) show a $\pi-\pi$ stacking with parallel discs (see Figure 5A). This stacking

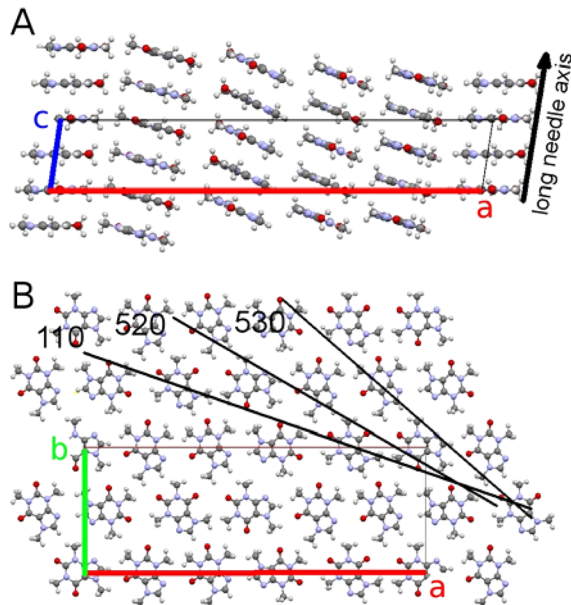


Figure 5. Views of the caffeine unit cell and molecule arrangement along the b -axis (A) and along the c -axis (B). 110, 520, and 530 denote the projection of contact planes.

direction coincides with the long needle axis of the crystallites. Along the a -axis the $\pi-\pi$ stacks are arranged which each stack being slightly inclined with respect to an adjacent. Along the b -axis the dislike caffeine molecules are packed in an ABA arrangement of equivalent sheets but with the B sheet translated half along the a -axes (see Figure 5B).

The X-ray investigation of the caffeine needles observed on the silica surface reveals a majority of crystallites having a 010 contact plane with the substrate surface. From this it follows that the caffeine molecules arrange favorably in an edge-on, standing conformation, meaning that the caffeine molecules adapt an arrangement with a minimum interaction area per molecule with the silica surface (see Figure 5A,B). The molecule arrangement of caffeine within the unit cell shows that an alternate sequence of the OH-groups and the terminal methyl groups is in contact with the silica surface. The rocking curve measurement reveals that the mosaicity of the 010 orientation is large and even small peaks are noted. This is in agreement with the pole figure measurements which show a much larger extension of the poles along the ψ -direction compared to the measurements performed on mica. This suggests that the silica surface introduces order during crystallization but the interaction strength is weak allowing

caffeine molecules to adapt with respect to the surface in a direction other than the 010 crystal net plane or stacking faults at the very interface region are present. Both result in rotated needles with the long needle axis (coinciding with the crystal c -axis) remaining parallel to the surface and an edge-on conformation of the caffeine molecules.

The measurements of caffeine crystals grown on mica surface reveal, similar to the silica surface, needle-like structures. Other than on the silica surface, however, the mica surface introduces an epitaxial order; i.e., defined textures together with defined azimuthal alignments prevail. The optical microscopy reveal several orientations which are 60° or 18° degrees inclined with respect to each other over the entire sample (compare Figure 2B). While the order of the crystal is easily obtained by the optical microscopy, no information on the relative arrangement with respect of the mica surface is accessible. Anyway, this information is obtained by the X-ray diffraction pole figure measurement which shows six double poles at constant ψ within a 360° turn of the sample.

For a complete understanding of this pole figure data a stereogram is best suited in which the orientational order of net plane normals (hkl) is compared to directional order of real space unit cells direction of the caffeine crystals ($[uvw]$) and the mica substrate ($[uvw]_m$) (see Figure 6). For sake of simplicity

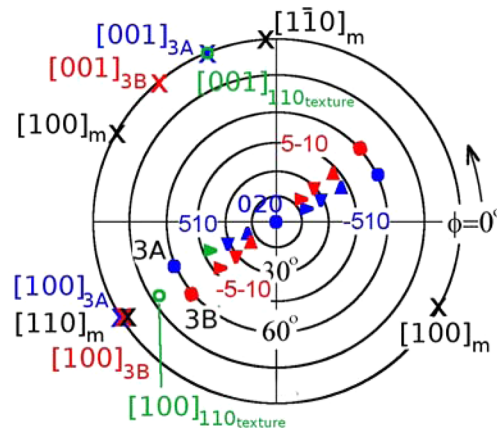


Figure 6. Stereogram for caffeine crystals on mica surfaces. Poles for caffeine needles resulting from a common texture are plotted with the same symbol; dots denote 020 texture, right-hand arrows denote 110 texture, upward arrows denote 520, and downward arrows denote 530 texture. $[uvw]_x$ denote the needle axis for different azimuthal crystal directions and $[uvw]_m$ denotes the mica real space crystal directions.

only poles for two azimuthal crystal directions, which are inclined by 18° in ϕ are explained in detail; this correspond to the poles 3A and 3B of Figure 4b,c. The poles located at $\phi = 24^\circ$ and 204° and $\psi = 60.5^\circ$ correspond to the 3A crystal alignment and are a result of caffeine crystals having a 010 contact plane; the enhanced pole densities correspond to the 510 and -510 net planes of caffeine (dots in Figure 6). From this the real space axis of caffeine can be deduced as the unit cell is known; both the direction of the a -axis ($[100]_{3A}$) and c -axis ($[001]_{3A}$) are in-plane ($\psi = 90^\circ$) at $\phi = 213^\circ$ and 114° , respectively. Comparing these results with the underlying mica substrate reveals that the caffeine crystal a -axis coincides with the $[110]_m$ direction of the mica substrate. This means that the “caffeine-discs” align along or very close to this direction in an edge-on conformation (compare Figure 5). The needle axis, which is (orientational) identical with the crystal c -axis, is 99° of

this direction and does not coincide with any main direction of the mica surface suggesting that the disc alignment is reason for the alignment.

The second azimuthal direction (3B, red dots in Figure 6) is a result of caffeine needles having a $\bar{0}10$ texture, meaning that the needle are flipped upside down. From this follows that the corresponding poles are the $\bar{5}10$ and $5\bar{1}0$ net planes. While the real space a -axis of this “flipped” texture ($[001]_{3B}$) coincides again with the $[110]_m$ direction of mica, the needle axis ($[001]_{3B}$) is inclined by 18° to the previous direction labeled as $[001]_{3A}$. For the understanding a scheme of this geometrical effect is provided in Figure 7a indicating the fact that inversion of the monoclinic unit with a subsequent alignment of the a -axis results in inclined growth direction of the needles.

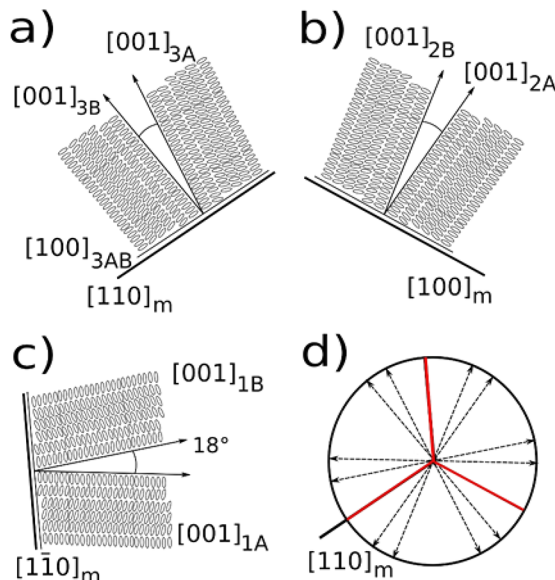


Figure 7. Schematics of the caffeine needle a -axis alignment with respect to the $[110]_m$ (a), the $[100]_m$ (b), and the $[1\bar{1}0]$ (c) real space direction of the mica substrate. (d) All needle growth directions (dashed arrows) together with the a -axis of the various directions.

The pole observed at $\psi = 41.5^\circ$ and $\phi = 204^\circ$ is a result of the caffeine needles having textures deviating from the 010 contact plane; a 110 texture is able to describe this pole (see Figure 6, right arrow). From this follows that the needles are rotated around the c -axis resulting in the needle preserving its needle direction along the surface; i.e., the $[001]$ caffeine directions for the 010 and 110 textures (and one azimuthal direction) coincide at $\psi = 90^\circ$ and $\phi = 114^\circ$. Consequently, the a -axis tilts from the surface pointing toward $\psi = 70.4^\circ$ and $\phi = 213^\circ$ (see circle in Figure 6). A comparison with the unit cell in Figure 5B reveals that the edge-on conformation of the molecules remains intact for this 110 texture, and an alternating sequence of the oxygen and terminal methyl group is in contact with the surface. In the same fashion the poles at $\psi = 20^\circ$ or 30.6° result from 520 and 530 textures, respectively. The a -axes are inclined by $\psi = 49^\circ$ and 60° from the surface normal and all c -axis coincide at $\psi = 70.4^\circ$ and $\phi = 213^\circ$. Due to the low resolution of the experimental setup, both reflections (020 and 510) are accessible within one pole figure taken at 8.4 nm^{-1} . This allows other textures to be found which results in 020 reflections coinciding with the poles in Figure 6. However, for all caffeine needle textures the a -axis azimuthal direction align

along the $[110]_m$ direction of the mica substrate, and thus the discs align along this direction. The edge-on conformation prevails for all these textures which most likely results from the dislike nature of the caffeine molecules.

The inspection of the pole figure reveals four additional needle directions (1A, 1B, 2A, and 2B, in Figure 4b,c) on the mica surface. Similar to the $[100]_{3A}$ and $[100]_{3B}$ axis the a -axis of the other crystal direction shows coinciding a -axis along the other main direction which is $\pm 120^\circ$ rotated from the $[110]_m$ direction; the $[100]_{2A}$ and $[100]_{2B}$ axes align along $[100]_m$ (Figure 7b), and the $[100]_{1A}$ and $[100]_{1B}$ axis align along $[1\bar{1}0]_m$ (Figure 7c). The needle axes of adjacent needle directions are again inclined by 18° with respect to each other. In Figure 7d all directions observed within the experiments are summarized. Typically for mica surface a pseudo 120° symmetry is observed for the alignment of the caffeine a -axis within the mica surface. Furthermore the growth direction shows a mirror symmetry with respect to the $[110]_m$ direction.

5. CONCLUSION

The experiments show the surface mediated growth of the nonsymmetric and disc-like caffeine molecules into needles on silica and mica surfaces. Up to now the main focus of structural investigation was centered around highly symmetric molecules with only very few exceptions on asymmetric ones. Here we have shown that the highly asymmetric molecule caffeine is able to compete with the solvent molecules for adsorption sites at the substrate surface and an edge-on alignment of the molecules with respect to the surface results. While on both substrates needles are aligned along the surface, rotational freedom along the needle axis results in various contact planes with the substrates. The in-plane (azimuthal) alignment depends on the symmetry or periodicity of the substrate. On the isotropic silica substrate needles grow randomly with no preferred azimuthal direction. On mica the regular arrangement of the surface atoms introduces constraints which dictate crystallization along certain directions. While needles do not grow along the high symmetry direction of the mica surface, the caffeine “discs” arrange along the main axes of mica ($[110]_m$, $[100]_m$, and $[1\bar{1}0]_m$) suggesting favored interaction is present along these directions.

Typically, mica surfaces provide besides defined surface symmetry also geometrical constraints by lowered oxygen atoms which results in the presence of microgrooves along the $[110]_m$ direction, which often induces a preferred alignment of crystallites with respect to this direction. The caffeine a -axis alignment reveals that three directions are present which have a 120° inclination with respect to each other, suggesting growth is very similar in all directions. Surprisingly, however, the grooves do not induce any constraint for the alignment of the caffeine needles at the surface, which suggests that the geometrical constraint is of no or only minor importance for the crystal growth direction within the studied system.

■ ASSOCIATED CONTENT

Supporting Information

Pole figures of caffeine crystal on a silica surface and mica surface. This material is available free of charge via the Internet at <http://pubs.acs.org>.

■ AUTHOR INFORMATION

Corresponding Author

*E-mail: oliver.werzer@uni-graz.at.

Notes

The authors declare no competing financial interest.

■ REFERENCES

- (1) Pardeike, J.; Weber, S.; Haber, T.; Wagner, J.; Zarfl, H. P.; Plank, H.; Zimmer, A. *Int. J. Pharm.* **2011**, *419*, 329.
- (2) Ozdemir, M.; Yurteri, C. U.; Sadikoglu, H. *Crit. Rev. Food Sci. Nutr.* **1999**, *39*, 457.
- (3) Werzer, O.; Atkin, R. *Phys. Chem. Chem. Phys.* **2011**, *13*, 13479.
- (4) Werzer, O.; Warr, G. G.; Atkin, R. *Langmuir* **2011**, *27*, 3541.
- (5) Nabok, D.; Puschnig, P.; Ambrosch-Draxl, C.; Werzer, O.; Resel, R.; Smilgies, D. *Phys. Rev. B* **2007**, *76*, 235322.
- (6) Werzer, O.; Stadlober, B.; Haase, A.; Oehzelt, M.; Resel, R. *Eur. Phys. J. B* **2008**, *66*, 455.
- (7) Acharya, S.; Sahoo, S. K. *Adv. Drug Delivery Rev.* **2011**, *63*, 170.
- (8) Bala, I.; Hariharan, S.; Kumar, M. N. *Crit. Rev. Ther. Drug Carrier Syst.* **2004**, *21*, 387.
- (9) Won, Y. W.; Kim, Y. H. *J. Controlled Release* **2008**, *127*, 154.
- (10) Li, W.-M.; Liu, D.-M.; Chen, S.-Y. *J. Mater. Chem.* **2011**, *21*, 12381.
- (11) Fröhlich, E.; Meindl, C.; Roblegg, E.; Griesbacher, A.; Pieber, T. R. *Nanotoxicology* **2012**, *6*, 424.
- (12) Roblegg, E.; Fröhlich, E.; Meindl, C.; Teubl, B.; Zaversky, M.; Zimmer, A. *Nanotoxicology* **2012**, *6*, 399.
- (13) *Springer Handbook of Nanotechnology*; Bhushan, B., Ed.; Springer: Berlin, 2006.
- (14) Stadlober, B.; Haas, U.; Maresch, H.; Haase, A. *Phys. Rev. B* **2006**, *74*, 165302 (1).
- (15) Werzer, O.; Matoy, K.; Smilgies, D.; Rothmann, M.; Strohriegl, P.; Resel, R. *J. Appl. Polym. Sci.* **2007**, *107*, 1817.
- (16) Kinder, L.; Kanicki, J.; Petroff, P. *Synth. Met.* **2004**, *146*, 181.
- (17) Kumar, S.; Kim, J.-H.; Shi, Y. *Phys. Rev. Lett.* **2005**, *94*, 077803.
- (18) Putsche, B.; Tumbek, L.; Winkler, A. *J. Chem. Phys.* **2012**, *137*, 134701(1).
- (19) Tumbek, L.; Winkler, A. *Surface Sci.* **2012**, *606*, 55.
- (20) Gerlach, A.; Hosokai, T.; Duhm, S.; Kera, S.; Hofmann, O.; Zojer, E.; Zegenhagen, J.; Schreiber, F. *Phys. Rev. Lett.* **2011**, *101*, 156102.
- (21) Haber, T.; Resel, R.; Andreev, A.; Oehzelt, M.; Smilgies, D.-M.; Sitter, H. *J. Cryst. Growth* **2010**, *312*, 333.
- (22) Haber, T.; Ivanco, J.; Ramsey, M. G.; Resel, R. *J. Cryst. Growth* **2008**, *310*, 101.
- (23) Resel, R. *J. Phys. Cond. Mater.* **2008**, *20*, 184009.
- (24) Wedl, B.; Resel, R.; Leising, G.; Kunert, B.; Salzmann, I.; Oehzelt, M.; Koch, N.; Vollmer, A.; Duhm, S.; Werzer, O.; Gbabode, G.; Sferrazza, M.; Geerts, Y. H. *RSC Adv.* **2012**, *2*, 4404.
- (25) Birkholz, M. *Thin Film Analysis by X-ray Scattering*; Weinheim: Wiley-VCH, 2006.
- (26) Resel, R.; Lengyel, O.; Haber, T.; Werzer, O.; Hardeman, W.; de Leeuw, D.; Wondergem, H. *J. Appl. Crystallogr.* **2007**, *40*, 580.
- (27) Salzmann, I.; Resel, R. *J. Appl. Crystallogr.* **2004**, *37*, 1029.
- (28) Lehmann, C. W.; Stowasser, F. *Chem.—Eur. J.* **2007**, *13*, 2908.
- (29) Gorelik, T.; Sarfraz, A.; Kolb, U.; Emmerling, F.; Rademann, K. *Cryst. Growth Des.* **2012**, *12*, 3239.
- (30) Sarfraz, A.; Simo, A.; Fenger, R.; Christen, W.; Rademann, K.; Panne, U.; Emmerling, F. *Cryst. Growth Des.* **2012**, *12*, 583.
- (31) Sutor, D. *J. Acta Crystallogr.* **1985**, *11*, 453.
- (32) Senden, T. J.; Drummond, C. *J. Colloids Surf.* **1995**, *94*, 29.
- (33) Simbrunner, C.; Nabok, D.; Hernandez-Sosa, G.; Oehzelt, M.; Djuric, T.; Resel, R.; Romaner, L.; Puschnig, P.; Ambrosch-Draxl, C.; Salzmann, I.; Schwabegger, G.; Watzinger, I.; Sitter, H. *J. Am. Chem. Soc.* **2011**, *133*, 3056.
- (34) Simbrunner, C.; Hernandez-Sosa, G.; Oehzelt, M.; Djuric, T.; Salzmann, I.; Brinkmann, M.; Schwabegger, G.; Watzinger, I.; Sitter, H.; Resel, R. *Phys. Rev. B* **2011**, *83*.
- (35) Boistelle, R.; Astier, J. P. *J. Cryst. Growth* **1988**, *90*, 14.